EMPIRICAL MODE DECOMPOSITION BASED DENOISING TECHNIQUES

Yannis Kopsinis, Stephen (Steve) McLaughlin

IDCOM,School of Engineering and Electronics
The University of Edinburgh, King's Buildings, EH9 3JL, Edinburgh

ABSTRACT

One of the most challenging tasks for which EMD could be useful is that of non-parametric signal denoising, an area in which wavelet thresholding has been the dominant technique for many years. In this paper, the major wavelet thresholding principle is used in the decomposition modes resulting from applying EMD to a signal. We show, that although a direct application of this principle in the EMD case is not feasible, it can appropriately adapted by exploiting the special characteristics of the EMD decomposition modes. In the same manner, inspired by the translation invariant wavelet thresholding, a similar technique adapted to EMD is developed leading to enhanced denoising performance.

1. INTRODUCTION

The Empirical mode decomposition (EMD) method [1] is an algorithm for the analysis of multicomponent signals [2] that works by breaking the signal into a number of amplitude and frequency modulated (AM/FM) zero mean signals, termed intrinsic mode functions (IMFs). In contrast to conventional decomposition methods such as wavelets, which perform the analysis by projecting the signal under consideration onto a number of predefined basis vectors, EMD expresses the signal as an expansion of basis functions which are signal-dependent, and are estimated via an iterative procedure called sifting.

Although many attempts have been made to increase the understanding of the way EMD operates and to improve its performance (see for example [3], [4], [5], [6], [7]), EMD still lacks a sound mathematical theory and is essentially described by an algorithm. However, partly due to the fact that it is easily and directly applicable and partly because it often results in interesting and useful decomposition outcomes, it has found a vast number of diverse applications such us biomedical [8], [9], watermarking [10] and audio processing [11] to name a few.

Apart from the topic specific applications of EMD listed above, a more generalized task in which EMD can be proved useful is signal denoising. In this paper, inspired by standard wavelet thresholding and translation invariant thresholding, EMD-based denoising techniques are developed and tested in many different signal scenarios. We show, that although the main principles shared by wavelet and EMD thresholding remain the same, in the case of EMD, the thresholding operation has to be properly adapted in order to be consistent with the special characteristics of the signal modes that result from EMD.

This work was performed as part of the BIAS consortium under a grant funded by the EPSRC under their Basic Technology Programme.

2. EMD: A BRIEF DESCRIPTION AND NOTATION

Empirical mode decomposition (EMD)[1] adaptively decomposes a multicomponent signal [2] $x(t)$ into L Intrinsic Mode Functions (IMFs), $h^{(i)}(t),\ 1 \leq i \leq L$,

$$x(t) = \sum_{i=1}^{L} h^{(i)}(t) + d(t). \tag{1}$$

where $d(t)$ is a non zero-mean low order polynomial remainder. Each one of the IMFs, say the ith one $h^{(i)}(t)$, is estimated with the aid of an iterative process, called sifting, applied to the residual multicomponent signal

$$x^{(i)}(t) = \begin{cases} x(t) & , i = 1 \\ x(t) - \sum_{j=1}^{i-1} h^{(j)}(t) & , i \geq 2 \end{cases} \tag{2}$$

The sifting process is effectively an empirical nevertheless powerful technique for the estimation of the local mean $m^{(i)}(t)$ of the residual multicomponent signal $x^{(i)}(t)$. Although the term *local mean* is, especially for multicomponent signals, somewhat vague, in the EMD context means that its substraction from $x^{(i)}(t)$ will lead to a signal, which is actually the corresponding IMF, i.e. $h^{(i)}(t) = x^{(i)}(t) - m^{(i)}(t)$, that is going to have the following properties:

1. Zero mean.
2. All the maxima and all the minima of $h^{(i)}(t)$ will correspondingly be positive and negative.
3. $h^{(i)}(t)$ will be narrowband but not necessarily monocomponent allowing the existance of both amplitude and frequency modulation (AM/FM).

By construction, the number of, say $N(i)$, extrema of $h^{(i)}(t)$ positioned in time instances $\boldsymbol{r}^{(i)} = [r_1^{(i)},\ r_2^{(i)}, \ldots,\ r_{N(i)}^{(i)}]$ and the corresponding IMF points $h^{(i)}(r_j^{(i)}),\ j = 1,\ \ldots,\ N(i)$, will alternate between maxima and minima, i.e., positive and negative values. As a result, in any pair of extrema, $\boldsymbol{r}_j^{(i)} = [h^{(i)}(r_j^{(i)}), h^{(i)}(r_{j+1}^{(i)})]$, corresponds a single zero-crossing $z_j^{(i)}$. Depending on the IMF shape, the number of zero-crossings can be either $N(i)$ or $N(i)-1$. Moreover, each IMF, e.g. of order i, have fewer extrema than all the lower order IMFs, $j = 1, \ldots,\ i-1$, leading to fewer and fewer oscillations as the IMF order inceases. In other words, each IMF occupies lower frequencies locally in the time-frequency domain than preceding ones.

Fig. 1 depicts, as an example, the outcome of the application of EMD to a well studied piecewise-regular signal [12] (Fig. 1a) corrupted by white Gaussian noise corresponding to a 5dB signal to noise power ratio (SNR). EMD results in 11 IMFs shown in Fig. 1b-l.

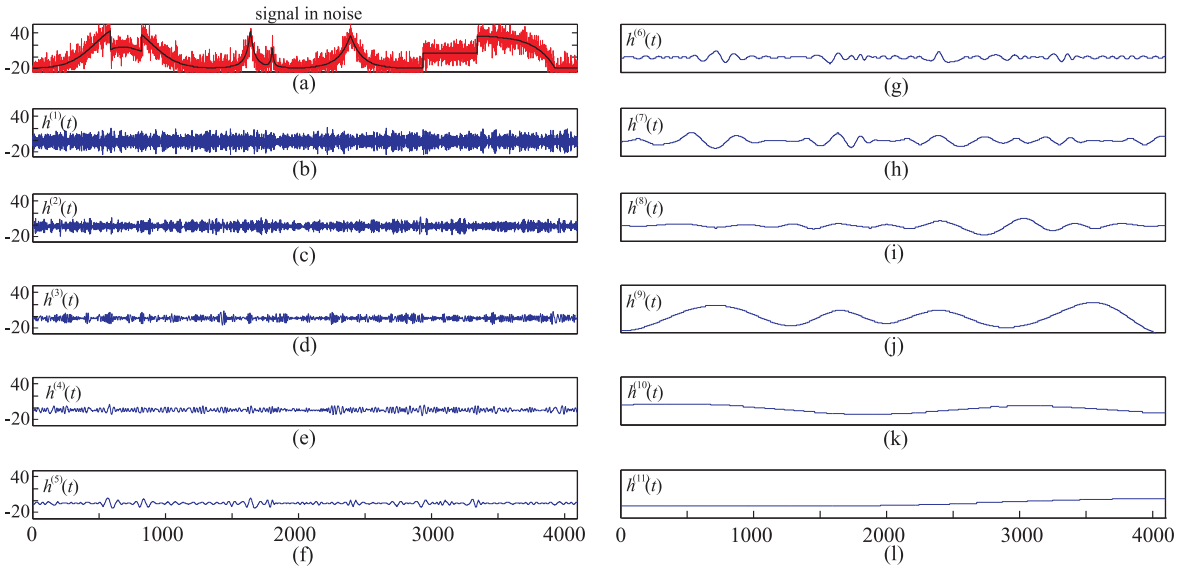

Fig. 1. Empirical mode decomposition of a noisy signal

3. SIGNAL DENOISING

Signal denoising can be described as follows:

Having sampled a noisy signal $x(t)$ given by $x(t) = \bar{x}(t) + \sigma n(t)$, $t = 1, 2, \ldots, N$ where, $\bar{x}(t)$ is the noiseless signal and $n(t)$ are independent random variables Gaussian distributed $\mathcal{N}(0, 1)$, produce an estimate $\tilde{x}(t)$ of signal $\bar{x}(t)$. Noise variance σ can be known or unknown and the denoising methods can be categorized as parametric or non-parametric depending on whether a predefined parametric model of $\bar{x}(t)$ is adopted or not. In this paper, we are focussing on the non-parametric framework where the best known candidates are denoising techniques based on wavelet decomposition [12], [13], [14]. Moreover, the novelty of this paper is the introduction of new non-parametric thresholding techniques applied to the decomposition modes resulting from EMD instead of the wavelet components. As will be seen, thresholding in EMD, is not a straightforward application of the concepts used in wavelet thresholding.

3.1. Wavelet based denoising

Employing a chosen orthonormal wavelet basis, an orthogonal $N \times N$ matrix $\boldsymbol{W}$ is appropriately built [15] which in turn leads to the discrete wavelet transform (DWT)

$$\boldsymbol{c} = \boldsymbol{W}\boldsymbol{x}$$

where, $\boldsymbol{x} = [x(1),\ x(2), \ldots,\ x(N)]$ and $\boldsymbol{c} = [c_1,\ c_2, \ldots,\ c_N]$ contains the resultant wavelet coefficients. Due to the orthogonality of matrix $\boldsymbol{W}$, any wavelet coefficient c_i follows normal distribution with variance σ and mean the corresponding coefficient value $\bar{c}_i$ of the DWT of the noiseless signal $\bar{x}(t)$. Provided that the signal under consideration is sparse in the wavelet domain, which is actually the case with the most of the signals we are interested in, then the DWT is expected to distribute the total energy of $\bar{x}(t)$ in only a few wavelet components lending themselves to high amplitudes. As a result, the amplitude of the most of the wavelet components is attributed to noise only. The fundamental reasoning of wavelet thresholding is to set to zero all the components which are lower than a threshold related to noise level, i.e., $T = \sigma C$, where C is a constant, and then reconstruct the denoised signal $\tilde{x}(t)$ utilizing the high amplitude components only. The hard thresholding operator is defined by

$$\rho_T(y) = \begin{cases} y, & |y| > T \\ 0, & |y| \leq T, \end{cases} \tag{3}$$

Consequently, the estimated denoised signal is given by

$$\tilde{\boldsymbol{x}} = \boldsymbol{W}^T \tilde{\boldsymbol{c}} \tag{4}$$

where, $\tilde{\boldsymbol{c}} = [\rho_T(c_1),\ \rho_T(c_2),\ \ldots,\ \rho_T(c_N)]$ and $\boldsymbol{W}^T$ denotes transposition of matrix $\boldsymbol{W}$. Apart from the standard wavelet thresholding described above, a number of modifications are investigated in our simulation results section including translation invariant thresholding [12] and Bayesian-based wavelet thresholding [16], [13].

With respect to the threshold selection, the universal threshold $T = \sigma\sqrt{2 \ln N}$ is a popular candidate. Such a threshold guarantees with high probability that all the components attributed to noise will have lower amplitudes. In this paper, multiples of the above threshold are used and the noise variance is estimated using a robust estimator based on the median of the components [12]. Moreover, it is usually beneficial to apply thresholding after a primary resolution level leaving the coarse scales corresponding to low frequencies unthresholded. This parameter will be taken into account in our study.

Fig. 2a,b shows the noise-free estimates of the corrupted by noise signal of Fig. 1 using wavelet hard thresholding with the universal threshold and Bayesian-based wavelet thresholding. The numbers on the top left of the figures indicates the SNRs after the denoising procedure. Note that this performance corresponds to a single arbitrary noise realization.

3.2. Conventional EMD denoising

The initial attempt at using EMD as a denoising tool emerged from the need to know whether a specific IMF contains useful information or primarily noise. Thus, significance IMF test procedures were simultaneously developed both by Flandrin et. al. [17], [18] and Wu et. al. [19], [20] based on the statistical analysis of modes resulted from the decomposition of signals consisting solely of fractional Gaussian noise and white Gaussian noise respectively. The

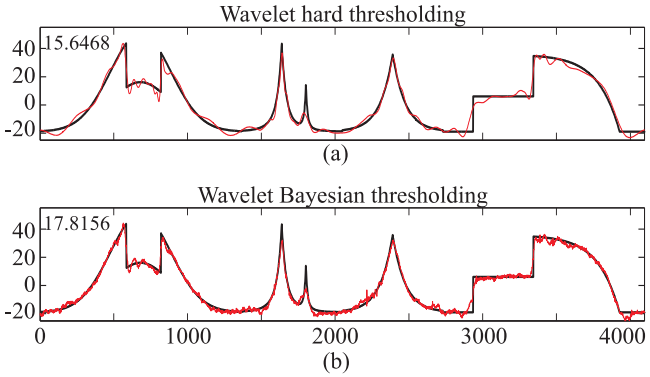

Fig. 2. Examples of Wavelet-based denoising. The top-left numbers are the SNR values after denoising.

reasoning underlying the above significance test procedure is fairly simple but strong. If one knows the energy of the IMFs resulting from the decomposition of a noise-only signal with certain characteristics, then in actual cases of signals comprising both information and noise with the specific characteristics, a significant discrepancy between the energy of a noise-only IMF and the corresponding noisy-signal IMF indicates the presence of useful information. In a denoising scenario this translates to partially reconstructing the signal using only the IMFs which contain useful information and discarding the IMFs that carry primarily noise, i.e., the IMFs that share similar amounts of energy with the corresponding noise-only case.

In practice the noise-only signal is never available in order to apply EMD and estimate the IMF energies, so the usefulness of the above technique relies on whether or not the energies of the noise-only IMFs can be estimated directly based on the actual noisy-signal. The latter is usually the case due to a striking feature of EMD. Apart from the first noise-only IMF, the power spectra of the other IMFs exhibit self similar characteristics similar to those which appear in any dyadic filter structure. As a result, the IMF energies, E_k should linearly decrease in a semi-log diagram of, e.g., $\log_2 E_k$ with respect to k. It also turns out that the first IMF carries the higher amounts of energy. In this paper we will focus in signals with white Gaussian noise. Then, the noise-only IMF energies can be approximated according to the equation [18]:

$$\hat{E}_k = \frac{\hat{\sigma}_n^2}{0.719} 2.01^{-k},\ k = 2,\ 3,\ 4, \ldots \tag{5}$$

where, $\hat{\sigma}_n^2$ is the noise variance which can be approximated with the variance of the first IMF.

Fig. 3 deals with the conventional denoising of the test signal of Fig. 1a. On top, with solid line we see the semilog diagram (energies with respect to IMF number) of the corresponding IMFs (Fig. 1b-l) and the dashed line shows the results of the noise only model of (5). We observe that after the fifth IMF the energies significantly diverge from the theoretical model indicating the presence of significant amounts on no-noise signal. The partial signal reconstruction including only IMF number 6 to 11 results in the denoised signal shown in Fig. 3.

4. IMF THRESHOLDING-BASED DENOISING

An alternative EMD denoising is proposed in this paper inspired by wavelet thresholding. Some preliminary results have already appeared very recently in [21], [22], [23] where the wavelet thresholding idea is directly applied to the EMD case. However, it will be seen that EMD-thresholding can exceed the performance achieved by wavelet thresholding only by adapting the thresholding function to the special nature of IMFs.

EMD performs a subband like filtering resulting in essentially uncorrelated IMFs. Although the equivalent filter-bank structure is by no means pre-determined and fixed as in wavelet decomposition, one can in principle perform thresholding in each IMF in order to locally exclude low energy IMF parts which are expected to be significantly corrupted by noise. A direct application of wavelet thresholding in the EMD case translates to:

$$\tilde{h}^{(i)}(t) = \begin{cases} h^{(i)}(t), & |h^{(i)}(t)| > T_i \\ 0, & |h^{(i)}(t)| \leq T_i, \end{cases} \tag{6}$$

where, $\tilde{h}^{(i)}(t)$ indicates the ith thresholded IMF. The reason for adopting different thresholds T_i per mode i will be discussed later on.

A generalized reconstruction of the denoised signal is given by

$$\tilde{x}(t) = \sum_{k=M_1}^{M_2} \tilde{h}^{(i)}(t) + \sum_{k=M_2+1}^{L} h^{(i)}(t) \tag{7}$$

where, the introduction of the parameters M_1 and M_2 gives us flexibility on the exclusion of the noisy low order IMFs and on the optional thresholding of the high order ones which in white Gaussian noise conditions contains low noise energy.

There are two major interconnected differences between wavelet and direct EMD thresholding (EMD-DT) as described in (6). First, in contrast to wavelet denoising where thresholding is applied to the wavelet components, in the EMD case, thresholding is applied to the N samples of each IMF which are basically the signal portion contained in each adaptive subband. An equivalent procedure in the wavelet method would be to perform thresholding on the reconstructed signals after performing the synthesis function on each scale separately. Secondly, as a consequence of the first difference, the IMF samples are not Gaussian distributed with variance equal to the noise variance as the wavelet components are irrespective of scale. In fact, the noise contained in each IMF is colored[1] *having different energy* in each mode. In that sense, EMD denoising is mostly related to wavelet denoising of signals corrupted by color noise where the thresholds have to be scale dependent [24]. In our study as thresholds we are going to use multiples of the IMF dependent universal threshold, i.e., $T_k = c\sqrt{E_k 2 \ln N}$, where c is constant. Moreover, the noise only IMF energies, E_k can be computed directly based on the variance estimate of the first IMF using (5).

4.1. Thresholding adapted to EMD characteristics

The direct application of wavelet like thresholding to the decomposition modes is in principle wrong and can have catastrophic consequences to the continuity of the reconstructed signal. This arises as a result of the special attributes that IMFs have, namely, they resemble an AM/FM modulated sinusoid with zero mean. As a result, it is guaranteed that, even in a noiseless case, in any interval $\boldsymbol{z}_j^{(i)} = [z_j^{(i)}\ z_{j+1}^{(i)}]$, the absolute amplitude of the ith IMF, $i = 1,\ 2, \ldots, N$, will drop below any non-zero threshold in the proximity of the zero-crossings $z_j^{(i)}$ and $z_{j+1}^{(i)}$. In other words, based

[1]There is strong evidence that at least in the noise-only case the distribution of the IMF samples is still Gaussian [20].

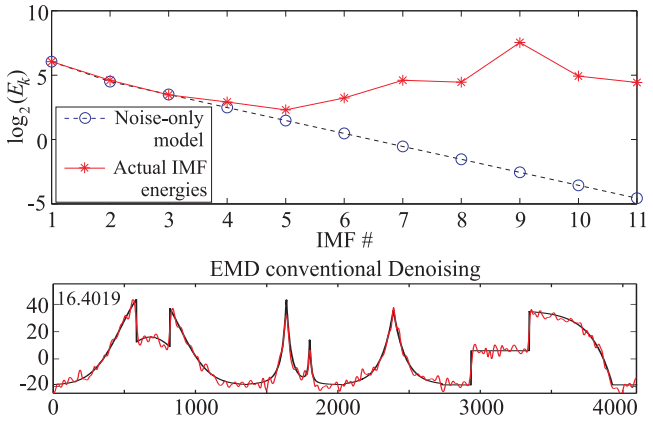

Fig. 3. (a) Theoretical noise-only model and actual IMF energies with respect to IMF number. (b) The resulted denoised signal when, for the reconstruction, the IMFs number 6 to number 11 are used only.

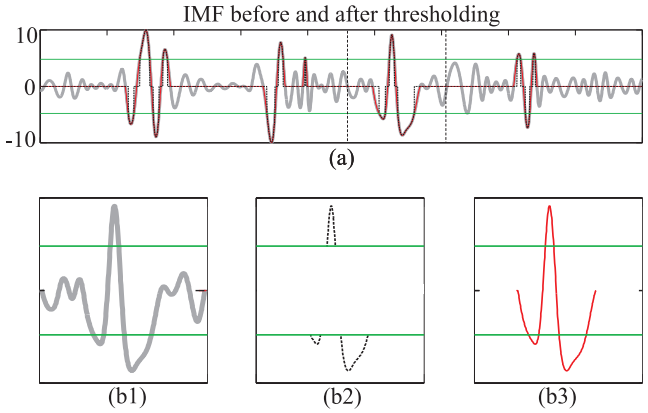

Fig. 4. Differences between Direct and Interval thresholding and the corresponding denoised signals.

on the absolute amplitude of isolated IMF samples is impossible to infer for any one of them if they correspond to noise or to useful signal. However, we are able to guess on whether the interval $\boldsymbol{z}_j^{(i)}$ is noise-dominant or signal-dominant based on the single extrema $h^{(i)}(r_j^{(i)})$ that corresponds to this interval. If the signal is absent, the absolute value of this extrema is going to lie below the threshold. Alternatively, in the presence of strong signal, the extrema value is expected to exceed the threshold. Moreover, since in each IMF the noise and the signal share the same bandwidth, the signal dominance at the extrema time instance is highly likely to be extended to all the IMF samples belonging to the specific zerocrossing interval. As a result the newly developed EMD hard thresholding, hereafter referred to as EMD interval thresholding (EMD-IT) which translates to:

$$\tilde{h}^{(i)}(\boldsymbol{z}_j^{(i)}) = \begin{cases} h^{(i)}(\boldsymbol{z}_j^{(i)}), & |h^{(i)}(r_j^{(i)})| > T_i \\ 0, & |h^{(i)}(r_j^{(i)})| \leq T_i, \end{cases} \tag{8}$$

for $j = 1, 2, \ldots, N_z^{(i)}$, where, $h^{(i)}(\boldsymbol{z}_j^{(i)})$ indicates the samples from instant $z_j^{(i)}$ to $z_{j+1}^{(i)}$ of the ith IMF and $N_z^{(i)}$ equals to either $N(i)$ or $N(i)-1$ depending on the ith IMF shape.

After careful consideration, it can be seen that the above procedure resembles wavelet thresholding more than direct EMD tresholding, because wavelet thresholding is applied to the wavelet coefficients. In fact, each coefficient is responsible for the values of a sequence of samples of the subsignal corresponding to the specific scale reconstruction which increases with scale and it is determined by the wavelet size of support. Similarly, the number of IMF samples which are altered or not in the EMD-IT depends on the IMF order and is increasing as the order increases.

Fig. 4a-b depicts the differences between the direct and the interval EMD thresholding. As an example, the sixth IMF of Fig. 1 has been used. The thick light colored line corresponds to the actual IMF and the solid and dotted line is associated with interval thresholding, and direct thresholding respectively. A detail of the thresholding function applied on the IMF segment shown between the two vertical dashed lines in Fig. 4a is also depicted in Fig. 4b1-b3. The horizontal lines indicates the plus and minus of the universal threshold. More specifically, in Fig. 4b2 and b3 we see the parts of the IMF segment which are not zero after thresholding. The discontinuities that EMD-DT introduces are apparent. EMD-IT reduces significantly such an effect. Fig. 5a and b show the denoising effect when the two different thresholding methods are used. We observe that for the same noise realization EMD-IT resulted in lower SNR than EMD-DT. It should be noted here, that the universal threshold is not the optimum one neither for EMD nor for wavelet thresholding as will become apparent in the simulations section.

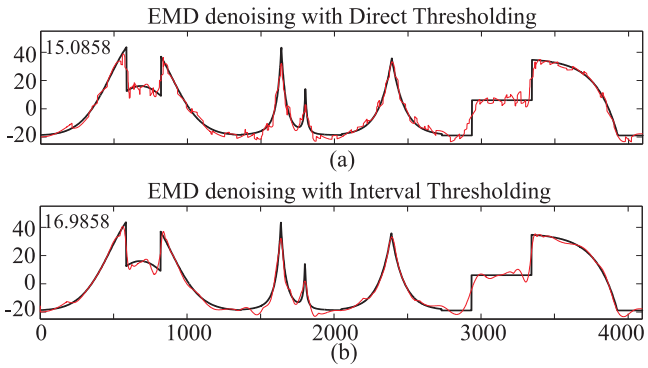

Fig. 5. Denoised signals after applying direct and interval thresholding.

4.2. Iterative EMD interval-thresholding

Inspired by translation invariant wavelet thresholding, where a number of denoised versions of the signal under consideration are obtained iteratively in order to enhance the tolerance against noise by averaging them, we make an attempt to develop an EMD-based denoising technique which exploits a similar principle. Once again, the direct application of translation invariant denoising to the EMD case will not work. This arises from the fact that the wavelet components of the circularly shifted versions of the signal correspond to atoms centered on different signal instances. In the case of the data-driven EMD decomposition, the major processing components, which are the extrema, are signal dependent leading to fixed relative extrema positions with respect to the signal when the latter is shifted. As a result, the EMD of shifted versions of the noisy signal corresponds to identical IMFs sifted by the same amount. Consequently, noise averaging can not be achieved in this way.

The different denoised versions of the noisy signal in the case of EMD can only be constructed from different IMF versions after being thresholded. Inevitably, this is possible only by decomposing different noisy versions of the signal under consideration itself. So the problem at hand translates to the following question: In which way, having a signal buried in noise, can you produce different noisy versions of the actual noise-free signal. The answer stems from within the EMD concept exploiting the characteristics of the first IMF. We know that in white Gaussian noise conditions, the first IMF is mainly noise. By circularly sifting by a random number of samples the first IMF and then adding the resulted noise signal to the sum of the rest of the IMFs we obtain a different noisy-version of the original signal. In fact, in case that the first IMF consist of noise only, then the total noise variance of the newly generated noisy-signal is the same to the original one.

The above EMD denoising technique, hereafter refered to as Iterative EMD interval-thresholding (EMD-IIT) is summarized in the following steps:

1. Perform an EMD expansion of the original noisy signal x.
2. Perform a partial reconstruction using the last $L-1$ IMFs only, $x_p(t) = \sum_{i=2}^{L} h^{(i)}(t)$.
3. Randomly circularly shift the sample positions of the first IMF, $h_a^{(1)}(t) = \text{CIRCSHIFT}(h^{(1)}(t))$.
4. Construct a different noisy version of the original signal, $x_a(t) = x_p(t) + h_a^{(1)}(t)$.
5. Perform EMD on the new altered noisy signal $x_a(t)$.
6. Perform the EMD-IT denoising (Eq. 8) to the IMFs of $x_a(t)$ to obtain a denoised version $\tilde{x}_1(t)$ of x.
7. Iterate between steps 3-6 $K-1$ times, where K is the number of averaging iterations in order to obtain k denoised versions of x, i.e., $\tilde{x}_1,\ \tilde{x}_2, \ldots, \tilde{x}_K$.
8. Average the resulted denoised signals $\tilde{x}(t) = \frac{1}{K}\sum_{k=1}^{K} \tilde{x}_k(t)$

5. SIMULATION RESULTS

Apart from the signal that was used in the previous section, the final simulations will be also performed with the Doppler signals shown in Fig. 6. The two signal used are sampled with different sampling

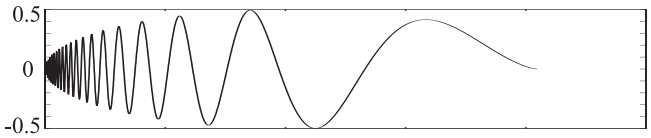

Fig. 6. Differences between Direct and Interval thresholding and the corresponding denoised signals.

periods in order to consist of 1024, 2048 and 4096 samples. The SNR values used are -2, 0 and 2 dB. The SNR values after the application of the denoising techniques discussed in this paper which corresponds to the ensemble average of 50 independent realizations per simulation setting, are shown in tables 1 and 2 for the piecewise-regular and Doppler signal respectively. The SNR values shown, corresponds to optimized values such as the primary resolution level for the wavelet based denoising techniques and parameters M_1, M_2 of equation (7) for the EMD based denoising. Moreover, the adopted wavelet filter is the symmlet of order 8 and in the case of EMD-IIT 20 iterations are used. Finally, for the methods that thresholding is applied, the best among 11 thresholds was adopted for each one of the different SNR/sampling frequency simulation setup. The 11 thresholds were calculated by multiplication of the universal threshold with the constants 0.4 up to 1.4 with steps of 0.1; It turned out that in both simulation examples and all the different simulation setups, the best threshold for EMD-IIT was between 0.5 to 0.7 times the universal threshold having small performance differences for any threshold between the above values. The picture is similar in the case of translation invariant thresholding with the difference that the optimum threshold values were between 0.7 and 0.9 times the universal threshold. We observe, that in almost all the cases EMD-IIT outperforms the rest of the methods. Moreover, the improvement increases with the increase of the sampling frequency.

6. CONCLUSIONS

In this paper, the basic wavelet thresholding operator was modified in order to suit to the special characteristics of EMD modes. Moreover, inspired by translation invariant wavelet thresholding, an iterative scheme for improved EMD denoising performance was developed. The new algorithms, have been tested with two well studied signals in high noise scenarios and their performance was compared with wavelet thresholding methods. It turned out, that the iterative EMD denoising method exhibit the best performance in most cases.

7. REFERENCES

[1] N. E. Huang et. al., "The empirical mode decomposition and the hilbert spectrum for nonlinear and non-stationary time series analysis," *Proc. R. Soc. Lond. A*, vol. 454, pp. 903–995, Mar. 1998.

[2] L. Cohen, *Time-Frequency Analysis*, Prentice Hall, 1995.

[3] P. Flandrin, G. Rilling, and P. Goncalves, "Empirical mode decomposition as a filter bank," *IEEE Signal Processing Lett.*, vol. 11, pp. 112– 114, Feb. 2004.

[4] G. Rilling and P. Flandrin, "One or two frequencies? the empirical mode decomposition answers," *IEEE Trans. Signal Processing*, pp. 85–95, Jan. 2008.

[5] Y. Washizawa, T. Tanaka, D. P. Mandic, and A. Cichocki, "A flexible method for envelope estimation in empirical mode decomposition," in *Knowledge-Based Intelligent Information and Engineering Systems, 10th International Conference, KES 2006, Bournemouth, UK*, 2006.

[6] Y. Kopsinis and S. McLauglin, "Investigation and performance enhancement of the empirical mode decomposition method based on a heuristic search optimization approach," *IEEE Trans. Signal Processing*, pp. 1–13, Jan. 2008.

[7] Y. Kopsinis and S. McLauglin, "Improved emd using doubly-iterative sifting and high order spline interpolation," *Journal on Advances of Signal processing (JASP)*, vol. 2008, Article ID 128293, 8 pages, 2008. doi:10.1155/2008/128293.

[8] Y. Zhang, Y. Gao, L. Wang, J. Chen, and X. Shi, "The removal of wall components in doppler ultrasound signals by using the empirical mode decomposition algorithm," *IEEE Trans. Biomed. Eng.*, vol. 9, pp. 1631–1642, Sept. 2007.

[9] L. Hadjileontiadis, "Empirical mode decompostion and fractal dimension filter," *IEEE Eng. Med. Biol. Mag.*, pp. 30 – 39, Jan. 2007.

Method	-2dB			0dB			2dB		
	1024	2048	4096	1024	2048	4096	1024	2048	4096
EMD-IIT	9.873	11.740	13.763	11.051	13.067	15.074	12.334	14.424	16.531
EMD-IT	8.755	10.591	12.280	9.844	11.853	13.688	11.249	13.078	15.064
EMD-DT	8.387	10.071	11.482	9.494	11.458	12.948	10.850	12.736	14.442
Hard-TI	8.686	10.328	11.894	10.121	11.783	13.465	11.462	13.429	15.134
Hard	9.569	11.092	12.601	10.742	12.290	13.675	12.096	13.262	15.066
Bayesian	9.745	11.406	13.296	11.083	12.661	14.608	12.388	13.933	15.968
EMD-conv	8.735	10.297	11.891	9.849	11.426	13.201	10.938	12.725	14.310

Table 1. SNRs after denoising the piece-wise regular signal.

Method	-2dB			0dB			2dB		
	1024	2048	4096	1024	2048	4096	1024	2048	4096
EMD-IIT	11.182	13.423	15.484	12.552	14.831	16.986	14.026	16.301	18.541
EMD-IT	9.448	11.606	13.535	10.799	12.887	15.241	12.366	14.359	16.676
EMD-DT	8.575	10.533	12.494	9.771	11.913	13.993	11.342	13.285	15.493
Hard-TI	9.806	11.543	13.300	11.607	13.609	15.290	13.568	15.538	17.157
Hard	8.959	10.566	12.624	10.764	11.907	14.465	12.681	13.466	16.156
Bayesian	9.739	11.563	13.721	11.352	13.054	15.412	12.951	14.629	17.087
EMD-conv	7.480	9.076	10.356	8.452	10.024	11.597	9.444	11.086	12.685

Table 2. SNRs after denoising the Doppler signal.

[10] B. Ning, S. Qiyu, Y. Zhihua H. Daren, and H. Jiwu, "Robust image watermarking based on multiband wavelets and empirical mode decomposition," *IEEE Trans. Image Processing*, pp. 1956 – 1966, Aug. 2007.

[11] Md. K. I. Molla and K. Hirose, "Single-mixture audio source separation by subspace decomposition of hilbert spectrum," *IEEE Trans. on Audio, Speech and Language Processing*, pp. 893 – 900, Aug. 2007.

[12] S. Mallat, *A wavelet tour of signal processing*, Academic press, second edition, 1999.

[13] A. Antoniadis and J Bigot, "Wavelet estimators in nonparametric regression: A comparative simulation study," *Journal of statistical software*, vol. 6, pp. 1–83, 2001.

[14] D. L. Donoho and I. M. Johnstone, "Ideal spatial adaptation by wavelet shrinkage," *Biometrika*, vol. 81, pp. 425–455, 1994.

[15] S. Theodoridis and K. Koutroumbas, *Pattern Recognition*, Academic press, third edition, 2006.

[16] H. C. Huang and N. Cressie, "Deterministic/stochastic wavelet decomposition for recovery of signal from noisy data," *Technometrics*, vol. 42, pp. 262–276, 2000.

[17] P. Flandrin, G. Rilling, and P. Gonçalvès, "Empirical mode decomposition as a filter bank," *IEEE Signal Processing Lett.*, vol. 11, pp. 112–114, Feb. 2004.

[18] P. Flandrin, G. Rilling, and P. Gonçalvès, *EMD equivalent filter banks, from interpetation to applications (in N. E. Huang and S. Shen, Hilbert-Huang Transform and Its Applications)*, World Scientific Publishing Company, first edition, 2005.

[19] Z. Wu and N. E. Huang, "A study of the characteristics of white noise using the empirical mode decomposition method," *Proc. Roy. Soc. London A*, vol. 460, pp. 1597–1611, June 2004.

[20] N. E. Huang Z. Wu, *Statistical significance test of intrinsic mode functions, (in N. E. Huang and S. Shen, Hilbert-Huang Transform and Its Applications)*, World Scientific Publishing Company, first edition, 2005.

[21] A. O. Boudraa and J. C. Cexus, "Denoising via empirical mode decomposition," in *ISCCSP2006*, 2006.

[22] Y. Mao and P. Que, "Noise suppression and flaw detection of ultrasonic signals via empirical mode decomposition," *Russian Journal of Nondestructive Testing*, vol. 43, pp. 196–203, 2007.

[23] T. Jing-tian, Z. Qing, T. Yan, L. Bin, and Z. Xiao-kai, "Hilbert-huang transform for ECG de-noising," in *1st International Conference on Bioinformatics and Biomedical Engineering (ICBBE 2007)*, 2007.

[24] I. M. Johnstone and B. W. Silverman, "Wavelet threshold estimators for data with correlated noise," *J. of the Royal Statistical Society. Series B*, vol. 59, pp. 319–351, 1997.